

Perspective: Acoustic metamaterials in transition

Ying Wu, Min Yang, and Ping Sheng

Citation: *Journal of Applied Physics* **123**, 090901 (2018);

View online: <https://doi.org/10.1063/1.5007682>

View Table of Contents: <http://aip.scitation.org/toc/jap/123/9>

Published by the *American Institute of Physics*

A dark blue banner with a background of glowing yellow and orange nodes connected by thin blue lines, resembling a network or molecular structure. The text is white and yellow.

Scilight

Sharp, quick summaries **illuminating**
the latest physics research

Sign up for **FREE!**

AIP
Publishing

Perspective: Acoustic metamaterials in transition

Ying Wu,¹ Min Yang,² and Ping Sheng^{2,a)}

¹*Division of Computer, Electrical and Mathematical Science and Engineering (CEMSE), King Abdullah University of Science and Technology (KAUST), Thuwal 23955-6900, Saudi Arabia*

²*Department of Physics, Hong Kong University of Science and Technology, Hong Kong, China*

(Received 2 October 2017; accepted 26 October 2017; published online 15 December 2017)

Acoustic metamaterials derive their novel characteristics from the interaction between acoustic waves with designed structures. Since its inception seventeen years ago, the field has been driven by fundamental geometric and physical principles that guide the structure design rules as well as provide the basis for wave functionalities. Recent examples include resonance-based acoustic metasurfaces that offer flexible control of acoustic wave propagation such as focusing and re-direction; parity-time (*PT*)-symmetric acoustics that utilizes the general concept of pairing loss and gain to achieve perfect absorption at a single frequency; and topological phononics that can provide one-way edge state propagation. However, such novel functionalities are not without constraints. Metasurface elements rely on resonances to enhance their coupling to the incident wave; hence, its functionality is limited to a narrow frequency band. Topological phononics is the result of the special lattice symmetry that must be fixed at the fabrication stage. Overcoming such constraints naturally forms the basis for further developments. We identify two emergent directions: Integration of acoustic metamaterial elements for achieving broadband characteristics as well as acoustic wave manipulation tasks more complex than the single demonstrative functionality; and active acoustic metamaterials that can adapt to environment as well as to go beyond the constraints on the passive acoustic metamaterials. Examples of a successful recent integration of multi-resonators in achieving broadband sound absorption can be found in optimal sound-absorbing structures, which utilize causality constraint as a design tool in realizing the target-set absorption spectrum with a minimal sample thickness. Active acoustic metamaterials have also demonstrated the capability to tune bandgaps as well as to alter property of resonances in real time through stiffening of the spring constants, in addition to the *PT* symmetric acoustics that can achieve unprecedented functionalities. These emergent directions portend the transitioning of the field from the stage of novelty demonstrations to imminent applications of some acoustic metamaterials to select real-world problems, supported by an active research endeavor that continues to push the boundary of possibilities. Published by AIP Publishing. <https://doi.org/10.1063/1.5007682>

INTRODUCTION

Acoustic metamaterials have experienced a continuous and robust development for over fifteen years. Initially defined as man-made structures with novel wave characteristics derived from local resonances,¹ the field has now been broadened to include all structures that display wave properties not found in nature. Looking back, we may characterize the initial beginning as a thought-liberating experience that broke some of the rules in the traditional paradigm of acoustics, thereby creating a large horizon for clever and imaginative explorations on the potential created by the mixture of geometry, materials, and waves. This article does not intend to review the whole field of acoustic metamaterials or its past development; such a task has already been performed very nicely by a multitude of review articles and books.²⁻⁶ Instead, our intention is to introduce some of the most recent works in this field and to attempt an appraisal on what may lie ahead.

A sustainable scientific development is usually propelled by the dual driver of curiosity and applications. During the

initial stage of acoustic metamaterials development, the focus was the negative values of mass density and bulk modulus, and the resulting extra functionalities that can be attained by such parameter values. We saw the breakdown of the traditional “limits” in the focusing, imaging, and the magnitude of reflection, attendant with the subwavelength size of the sample required to achieve such effects. Most of such effects were achieved through localized resonances, and the associated strong dispersive behavior dictates the narrow frequency character of these novel functionalities.

The advent of transformation optics^{7,8} and acoustics,⁹⁻¹¹ in association with the accessibility of all effective material parameter values in the wave equations, has led to an explosion of research activities that fully demonstrated the power of using mathematical rules to design the spatial distribution of material parameter for achieving a certain goal, such as cloaking. However, since the underlying metamaterials’ values are mostly achieved through local resonances, most of the transformation acoustic functionalities are also narrow frequency band in character.

More recently, much of the acoustic metamaterials research can be traced to the inspiration provided by the quantum electronic behavior in graphene. Prior to the advent

^{a)} Author to whom correspondence should be addressed: sheng@ust.hk

of graphene, the quantum nature of electrons is mostly confined to textbook knowledge since its experimental observations, such as mesoscopic phenomena, can be achieved by very few laboratories around the world. Graphene has dramatically changed this situation by making the quantum nature of electrons easily manifest, e.g., the quantum Hall effect,^{12,13} which would not be difficult to observe under a magnetic field of 5 T or larger. Since the Schrodinger's equation can be expressed in the form of Helmholtz equation for electrons with fixed energy, it follows that the novel effects predicted or seen in graphene should be reproducible by using time harmonic acoustic waves, also governed by the Helmholtz equation, with designed geometric structures. Such a realization has sparked a wave of graphene-inspired research activities that include the unusual Dirac-cone type of dispersion relation^{14–19} and its related effects, and topological one-way edge state. Even the effect of the magnetic field, which naturally couples to electron owing to its charge and which has no counterpart for acoustic waves, can be synthesized.^{20–25} It is well known that magnetic field breaks time-reversal symmetry in electronic systems. In acoustics, the time-reversal symmetry in wave propagation can be broken by a circular flow.²⁰

Dissipation is a ubiquitous effect in physical systems. It was known for a long time that when the dissipation exceeds a critical value, two coupled states in a Hamiltonian system would both display exponentially decaying behavior, with one state decaying much faster than the other by dumping part of its energy on the other state. Novel behavior that differs from the above has been achieved by adding energy into the system, i.e., gain instead of dissipation. Such so-called parity-time (*PT*) symmetric acoustics can display lossless (i.e., transparent) and non-symmetric propagation of acoustic waves.^{26–30}

In another important development, acoustic metasurfaces have joined their electromagnetic counterparts in the quest to manipulate electromagnetic and acoustic waves by using patterned 2D locally resonant structures.^{31,32} Local resonance is necessary in order to enhance the wave interaction with one layer of subwavelength structures.

In what follows, we review a small selection of recent works in acoustic metamaterials, defined in the broad sense of the term. The demands of real-world applications are then considered as the challenges to break the constraints of acoustic metamaterials, with potential solution approaches as some of the emergent future directions.

RECENT DEVELOPMENTS

Topological acoustics

Topology denotes the global property of geometric structures that remains unchanged under continuous deformation, such as stretching, crumpling, and bending. A coffee mug is topologically equivalent to a doughnut, but not a ball, because both the mug and the doughnut have a hole in their structures. It turns out that in two-dimensional free electron gas, the application of a perpendicular magnetic field can create, in reciprocal wavevector space, Brillouin zones with a non-zero number of holes. Such characteristics are

understood to underlie the quantized Hall effect, which in real space is associated with one-way conducting edge state in which the conducting electrons cannot be backscattered. The advent of graphene has not only made such 2D quantum electronic phenomena more accessible, but also ignited a wave of research efforts to reproduce such an effect in classical waves. In addition to the conducting edge state, the honeycomb lattice structure of graphene also implies that its wavefunction is necessarily in the form of a two-component vector, i.e., there are two degrees of freedom (usually denoted as pseudospin degrees of freedom), owing to the two carbon atoms per unit cell. In reciprocal wavevector space, the band structure has the rather unique characteristic of two cones touching at a point, denoted the Dirac cones, at six distinct wavevector positions in reciprocal space with three equivalent K points (sometimes called K valleys) and three equivalent K' points (K' valleys). Such richness in the graphene physical characteristics serves as the fertile ground for creating novel acoustic effects through designed structures.

Creating a structure for one-way flow of acoustic wave—analogue to the electronic edge state—is generally challenging because the linear acoustic wave equation is invariant under time-reversal operation. In other words, there is no analogue of magnetic field for acoustic waves. An acoustic rectifier design based on combining a linear attenuator and a carefully designed non-linear medium was implemented,^{33,34} but constraints like amplitude dependence limit its isolator applications.³⁵ Acoustic diodes made from linear materials showing asymmetric power transmission for particular input and output field distributions were designed as well,^{36–39} but these structures are not truly non-reciprocal.⁴⁰ However, a linear system containing a directional bias can exhibit non-reciprocity. This idea was implemented in acoustics by creating an acoustic analogue of Zeeman splitting in a meta-atom consisting of a compact resonant ring cavity with rotational air flow [Fig. 1(a)].²⁰ The rotational flow breaks the time-reversal symmetry, which was subsequently integrated with topological phases in acoustics to realize robust topologically protected one-way edge propagation of acoustic waves.^{21–23,25} Inspired by the quantum spin-Hall effect, people found that robust one-way edge states can also be achieved in systems without breaking the time-reversal symmetry. One example is the acoustic topological insulators created by acoustic crystals possessing double Dirac cones [Fig. 1(b)] in their reciprocal wavevector space. Without breaking the time-reversal symmetry, band inversion associated with the double Dirac cone occurs when the geometric parameters are varied, leading to the realization of pseudospin-dependent, one-way edge sound transports.^{41–43} Another example comes from the acoustic valley vortex states,¹⁷ which have both chirality and orbital angular momentum and were observed in sonic crystals with broken mirror-symmetry that lifts the degeneracy of K and K' valleys. Rotating anisotropic scatterers, shown in Fig. 1(c), were used to close and reopen the bandgaps, inducing the acoustic analogue of the topological semimetal-insulator transition. The so-called acoustic valley-Hall edge modes

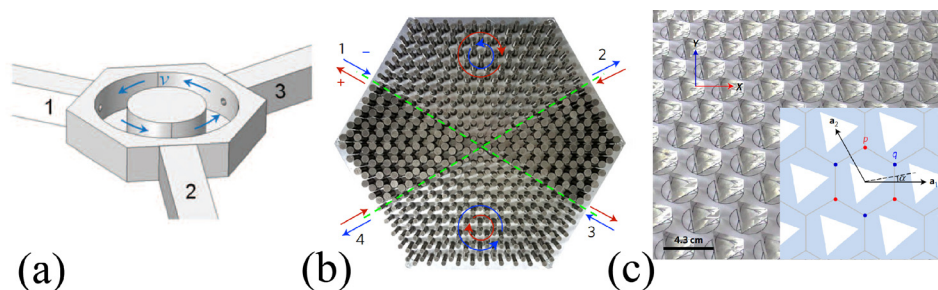


FIG. 1. (a) An acoustic meta-atom comprising a subwavelength acoustic ring resonator connected to three waveguides via three small holes. The circular motion of fluid in the ring resonator breaks the time-reversal symmetry, and provides the acoustic analogue of Zeeman splitting that lifts the degeneracy of counter-propagating resonance modes. Adapted from Ref. 20. (b) A cross-waveguide splitter made by arrays of steel cylinders in air. The upper and lower sections are formed by the topological phononic crystal (with smaller steel cylinders), and the left and right sections are formed by ordinary phononic crystal (with larger steel cylinders). Only a clockwise or counter-clockwise edge propagation on the interfaces is allowed for the acoustic pseudo-spin-up or pseudo-spin-down states. Adapted from Ref. 41. (c) A sonic crystal without mirror symmetry was used to observe the acoustic valley-Hall states. It is a triangular array of rotated triangular polymethyl methacrylate rods. Adapted from Ref. 44.

were demonstrated to be able to go around the sharply curved interface without reflection.⁴⁴

PT-symmetric acoustics

The modulation of the real part of acoustic parameters has witnessed great success in the initial stage of acoustic metamaterials development. Recently, this topic has been extended to the domain of the imaginary part of the acoustic parameters, related to dissipation. The consideration of acoustic characteristics in the complex parameter domain opens a door to the so-called non-Hermitian acoustics. Here, the term Hermitian refers to the mathematical property of the Hamiltonian matrix of the system that insures energy conservation. A Hermitian matrix has only real-valued eigenvalues. Non-Hermitian acoustics hence refers to those scenarios in which energy can be either dissipated or added. A non-Hermitian Hamiltonian matrix would generally have complex eigenvalues. An acoustic system is generally non-Hermitian, since the existence of loss is ubiquitous. Mathematically, it was observed that a non-Hermitian system that violates the time-reversal (T) symmetry (i.e., energy of the system dissipates as a function of time) but respects the combined parity (P)-time (T) symmetry (PT symmetry for short) can recover the real eigenvalue spectrum! This is so-called PT symmetric phase, and its property can differ from the usual Hermitian systems. By starting from a lossy system, a transition to a PT symmetric phase may be realized by tuning the loss or gain of the system. Exactly at the transition point, two complex-conjugate eigenvalues would coalesce, leading to an “exceptional point” singularity. The conceptual design of a PT -symmetric state was proposed in acoustics by Zhang and co-workers,²⁶ with the judicious choice of acoustic materials, attendant with carefully balanced loss and gain. Extraordinary scattering characteristics of the theoretically proposed acoustic PT medium were demonstrated from exact calculations, showing that the medium can exhibit unidirectional transparency at certain frequencies. A one-way cloak that protects its inner information from being detected only along a prescribed direction was further introduced by combining a PT -symmetric medium and transformation acoustics. However, the experimental

realization of the PT symmetric state is always accompanied by the challenge of designing an acoustic gain into the system so that there can be an effective imaginary part of the modulus exhibiting a sign that is opposite to the dissipative medium. Also, most gain and loss media required in PT symmetric systems are dispersive, thereby preventing them from fulfilling the stringent condition on the exact delicate balance of loss and gain over a broad frequency range. Considerable efforts have been devoted to the field of PT -symmetric acoustics. For example, the acoustic gain was designed and realized by a feedback system using the acoustic sound-controlling apparatus.⁴⁵ A pair of electro-acoustic resonators loaded with suitably tailored non-Foster electrical circuits [Fig. 2(a)] were used to synthesize a one-dimensional acoustic metamaterial cell whose effective density distribution respects the PT symmetry.²⁷ Such an acoustic device is capable of strongly sensing a signal via its passive component and is yet invisible. In addition to active electric amplification,^{27,28} coherent acoustic sources were exploited to generate a gain response that balances a passive loss.²⁹ The prototype consists of one loss cell and one gain unit, illustrated in Fig. 2(b). The loss cell is a waveguide carved with multiple slits to form a leaky region, and the gain unit comprises two acoustic source arrays, paired with upstream and downstream directive sensors. The use of active gain material to reach the PT symmetric condition is noted to be attainable over a reasonably broad frequency band, regardless of the lossy material’s dispersion characteristics. Thus, it is possible to access exceptional points at multiple frequencies. Recently, a PT -symmetric acoustic scattering was experimentally observed in an airflow duct with a pair of diaphragms.³⁰ Owing to the vortex-sound interaction, the flow in the diaphragms can effectively produce gain and loss [Fig. 2(c)]; and by fine-tuning the flow rate and the geometry of each diaphragm, the gain and loss can be adjusted. It is valid to say that the PT symmetric acoustics is a topic that is gaining momentum and followers.

Acoustic metasurfaces

The desire to manipulate acoustic waves on a subwavelength scale has always been a strong motivation from the

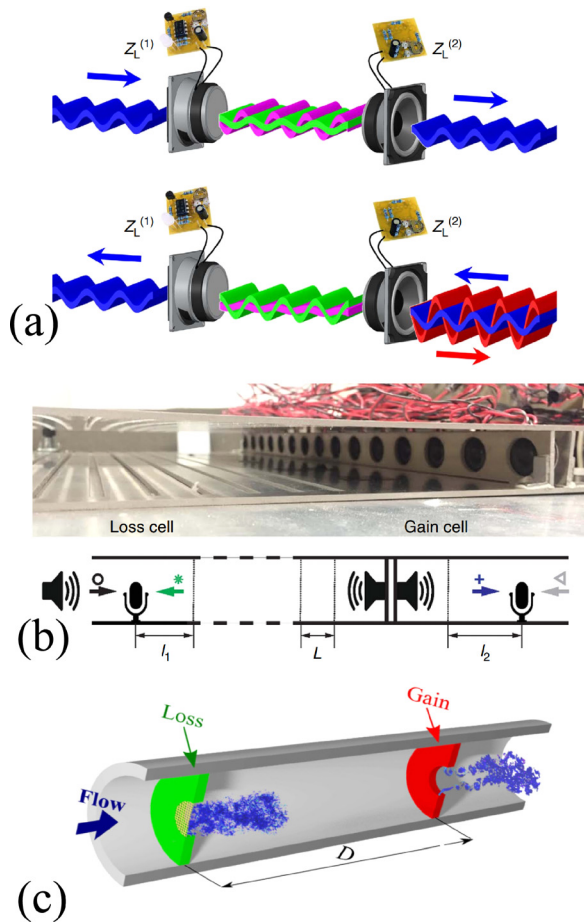


FIG. 2. Realizations of PT-symmetric acoustics. (a) A pair of loudspeakers loaded with properly tailored electric feedback circuits were used to tune the gain and loss. The left one is loaded with an absorptive circuit, functioning as the loss component, while the right one is loaded with an active electrical circuit tailored to realize a time-reversed version of the left one, forming an acoustic gain unit. The system has the property that it is transparent from the left, but highly reflective from the right. Adapted from Ref. 27. (b) A schematic diagram illustrating a system containing one lossy cell, with multiple slits carved in a waveguide to form a leaky region, plus one gain cell that contains two acoustic source-arrays paired with upstream and downstream (highly directive) sensors. Adapted from Ref. 29. (c) Two diaphragms in an airflow duct form two localized scattering units. One is associated with loss and the other corresponds to gain. The balance of loss and gain is realized by tuning the flow rate and geometry of each diaphragm. Adapted from Ref. 30.

beginning of acoustic metamaterials. This is especially true for sound in the audible range, where the wavelength can range up to the meter scale. In recent years, this direction has gained a new push from the emergence of acoustic metasurfaces. Metasurface is a term coined to denote planar structures, exhibiting ultra-subwavelength thickness that can retain functions that are central to devices such as lens, waveguides, and absorbers. The building units of acoustic metasurfaces can be resonant membranes,^{31,32,46} Helmholtz resonators, tube arrays,^{47–53} or space-coiling resonators.^{54–64} Below, we choose acoustic absorption as the functionality to survey this area.

Resonance enhances the local energy density, which is favorable to acoustic absorption since absorption is always the product of local energy density and the acoustic absorption coefficient, integrated over the sample volume. In this

context, the decorated membrane resonator (DMR) can highly localize the energy of incident sound around the edges of the rigid platelets.³² By means of membrane's intrinsic viscosity, the sound's energy can be efficiently dissipated within a thickness that is only 1/10 000 that of the relevant wavelength.^{32,65} However, dissipation by thin films is limited by geometric and symmetry constraints—only the sound component that matches the resonance symmetry can be coupled and absorbed.⁶⁵ Take the DMR for example. As the membrane is thin so that the relative motions between its two surfaces are frozen at low frequencies, its vibrations are always antisymmetric under mirror reflection. As sound incident from one-side can always be decomposed as a superposition of symmetric and antisymmetric components with the same amplitude, only half of its energy can couple to the DMR, implying a maximum absorption ratio of 50% [Ref. 65, Fig. 3(b)]. Similar limit also exists for resonators that are symmetric under mirror reflection, such as in the Helmholtz resonators mounted on the side wall of waveguide for airborne sounds,⁶⁶ or air bubbles embedded in rubber for waterborne sounds.⁶⁷ To overcome the 50% limit, the coherent perfect absorption (CPA) approach was proposed, in which a control wave, coherent with the incident wave, is launched from the opposite side [Fig. 3(a)]. By tuning the control wave in (out of) phase for the symmetric (antisymmetric) resonators, total absorption was achieved^{65,68} [Fig. 3(c)]. An alternative way to attain 100% absorption is to use a pair of degenerated resonators that have the two different symmetries at the same frequency.⁶⁹

The geometric and symmetry limits apply only to absorption in one scattering event. They can be broken by introducing multiple scatterings [Fig. 4(a)]. By backing the DMR with a reflecting plate, sound's energy can be almost completely absorbed at a frequency whose wavelength is over 100 times larger than the sample thickness³¹ [Figs. 4(b) and 4(c)]. In this particular case, a new hybrid resonance was created, characterized by a very large, non-radiative component of the membrane motion (which is responsible for the total absorption of the incident energy), and an average component, much smaller in amplitude, that can impedance-match with the incident wave. Similar total absorption can also be realized by placing the Helmholtz resonators in front of a hard surface,⁷⁰ or coiled acoustic Fabry-Pérot resonators.^{61,71}

Another application of acoustic metasurface is the generation of acoustic vortices, which have broad applications such as particle rotation manipulations induced by acoustic torque. The acoustic vortices are related to the acoustic orbital angular momentum, which is carried by wave fields with spiral phase dislocations described by an azimuthal phase $\exp(im\theta)$. Many efforts were devoted to the generation of acoustic waves with orbital angular momentum, such as acoustic source with radiating surface,⁷² phase-shifted transducer arrays and sparsely distributed acoustic transducer array,⁷³ and opto-acoustics.⁷⁴ Recently, new designs of acoustic vortex generator were proposed using metasurfaces. A planar layer of acoustic resonators comprising Helmholtz cavities and straight pipes was designed to generate acoustic vortex beams with orbital angular momentum.⁷⁵ Acoustic space-coiled unit cells were assembled to generate acoustic

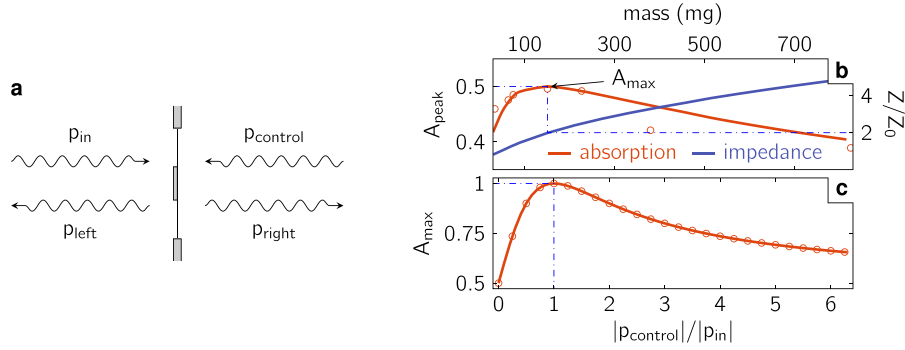


FIG. 3. Geometric constraint on sound absorption and coherent perfect absorption (CPA). (a) The realization of CPA by the decorated membrane resonator (DMR) that is an elastic membrane decorated by a rigid platelet. For an incoming wave with sound pressure amplitude p_{in} , the CPA approach introduces another control sound wave with $p_{control}$ from the opposite direction. The absorption ratio is given by $A = (|p_{left}|^2 + |p_{right}|^2) / (|p_{in}|^2 + |p_{control}|^2)$. (b) Under incoming sounds from one side, $p_{control} = 0$, the peak absorption (red curve) of the DMR is plotted as a function of the mass of the decorated platelets. The associated surface impedance (Z) is denoted by the blue curve. Here, the open circles are measured data, adapted from Yang *et al.*,⁶⁵ and the solid curve represents the theory. At the maximum absorption of 50%, the associated impedance is exactly twice that of air (Z_0). (c) Absorption of the DMR when waves are incident from two sides, plotted as a function of the relative amplitude ratio. Maximum absorption close to 1 occurs at $|p_{control}|/|p_{in}| = 1$, i.e., when the CPA condition is satisfied. Here, the open circles are numerical simulations, and the solid line is the theory prediction. Adapted from Ref. 65.

helical waves,⁷⁶ and multi-arm coiling slits were demonstrated to produce twisted stable acoustic vortices by modulating the amplitude and phase over a broad frequency band.⁷⁷ Applications to the manipulation of particles with acoustic radiation force and acoustic torque, exerted by an acoustic vortex beam, was reported thereafter.⁷⁸ The orbital angular momentum of acoustic vortex beams provides an extra dimension for coding and transmission of information. By utilizing the topological charges of orbital angular momentum, one order of magnitude enhancement in the data transmission rate has been demonstrated.⁷⁹

EMERGENT DIRECTIONS

Not all the research can result in commercial products, but the research efforts constitute the inevitable steps in a

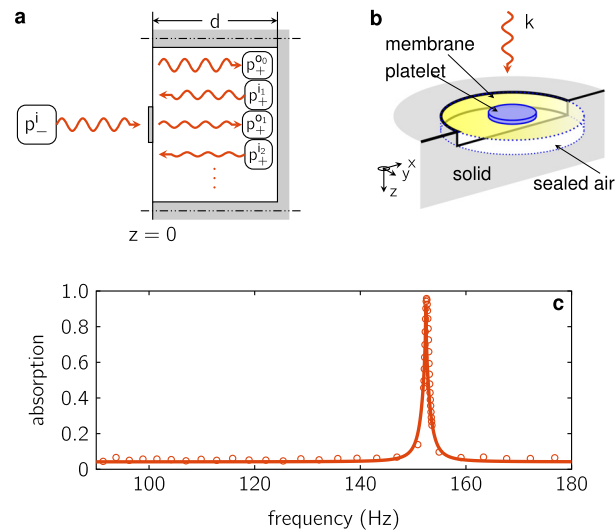


FIG. 4. Multiple scatterings and total sound absorption. (a) Schematic illustration of the multiple scatterings introduced by placing a reflecting wall closely behind a decorated membrane resonator (DMR). (b) Schematic illustration of a perfect absorber comprising a DMR backed by a very thin sealed air chamber with a reflecting back surface. This structure is shown to generate a hybrid resonance that can totally absorb the incident sound. (c) The absorption ratio of the DMR absorber. The solid curve is the theoretical prediction and the open circles are experimental data adapted from Ref. 31.

network of events leading to the eventual solution of real-world problems. Viewed in this context, acoustic metamaterials research is, on the one hand, entering a stage in which all the novel functionalities, uncovered so far, are undergoing some scrutiny as to their potential for advancing the technological backbone of our society. On the other hand, the creativity unleashed by the advent of metamaterials is moving the field to an ever-broadening horizon, limited only by human ingenuity. For this section, we focus on the former.

Local resonances underlie the majority of the novel functionalities attained by acoustic metamaterials; but they also constitute the one major shortcoming of being narrow frequency band in character. A natural way to extend the absorption bandwidth is to stack multiple resonances with frequencies slightly different from each other. Many attempts have been made along this direction;^{72–75} however, the lack of a central integration principle means that there can only be limited success. Recently, an integration strategy has emerged that can result in absorbers with true broadband character. The design recipe is guided by the causal constraint that relates the absorption spectrum of a sample to its thickness⁷⁶

$$d \geq \frac{1}{2\pi^2} \frac{B_{eff}}{B_0} \left| \int_0^\infty \ln[1 - A(\lambda)] d\lambda \right|, \quad (1)$$

where d is the sample thickness, B_{eff} is its effective bulk modulus at the static limit, B_0 is the air bulk modulus, and $A(\lambda)$ is the absorption coefficient as a function of wavelength λ . By setting two sides of Eq. (1) to be equal, the causal constraint can be turned into a design tool by which one may ask: For a given thickness, what is the best realizable absorption spectrum $A(\lambda)$? Or, for a target-set $A(\lambda)$, what is the minimum thickness attainable? The causal constraint relates the three most important aspects of acoustic absorption: the magnitude of the absorption, the relevant frequency band, and the sample thickness. In particular, it is noted that in the absence of sample thickness considerations, the issue of absorption becomes trivial.

By using a composite absorber with a multitude of Fabry-Pérot resonators, and by designing the resonance's

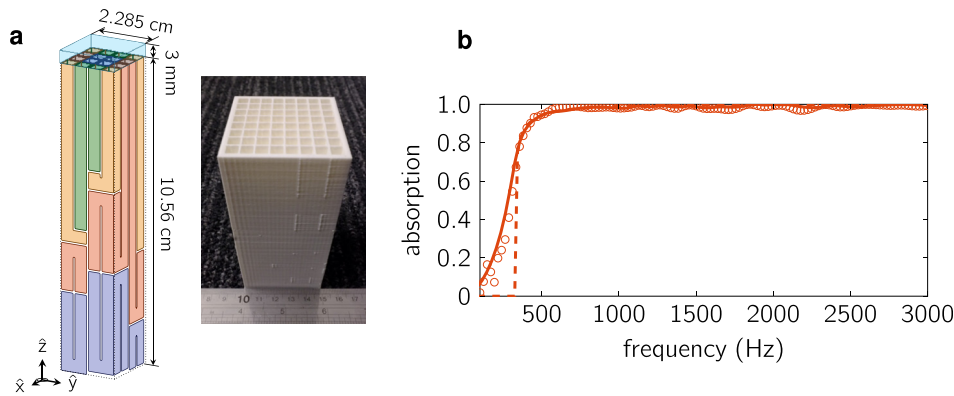


FIG. 5. Causally-optimal broadband absorber. (a) Schematics and photo image for the structure of the absorber. The absorber comprises 16 Fabry-Pérot channels with different lengths, folded into a compact cuboid. A very thin layer of sponge (cyan cube) was placed on the top of the acoustic metamaterial unit to provide dissipation through evanescent waves. The photo image shows the acoustic metamaterial unit, fabricated by 3D printing. (b) Absorption spectrum of the absorber. The solid line is from theoretical prediction and the open circles are experimental data. Adapted from Ref. 76.

mode density so as to best-match the surface impedance with that of air over a very broadband, a very flat absorption spectrum approaching unity has been realized, starting from a lower frequency cut-off. The wavelength of the lower frequency cut-off is an order of magnitude larger than the absorber thickness.⁷⁶ The resulting structure and the measured absorption spectrum are shown in Fig. 5.

The integration approach offers a versatile way to broaden the frequency range of applicability of some other functionalities. For example, if the acoustic metasurface can be made to be transparent to non-resonant frequencies, then multiple metasurfaces operating over different frequencies can be stacked together, thereby broadening the frequency range over which they can be effective as an integrated unit. Another obvious integration approach is to laterally tile the metamaterial units operating in different frequencies, and treat them as an integrated whole. In such an integration, it is inevitable that the problem of oscillator strength appears, since each local resonator, operating at a certain frequency, necessarily occupy a small fraction of the surface area. In the case of acoustic absorption, this problem is resolved by appealing to the causality constraint, through the consideration of the mode density of resonances.

Just as in the case electromagnetic metamaterials, tiling metamaterial units also offer the possibility of making the integrated unit active in character, through electrical control of each individual resonator. It should be noted that active acoustics has been around for a long time, and one can find many commercial products based on active control. The most well known of such active control is the cancellation of noise by first recognizing the signature of the acoustic noise, and then generating the necessary acoustic waves for its cancellation. Of course, active acoustics has now moved beyond this simple paradigm, with many of the new developments proprietary in nature. For acoustic metamaterials, active control is already emergent as an important direction.⁷⁷ Effective material parameters that are fundamentally not possible with passive materials are realized and even made to be actively tunable via external control.^{78,79} This is certainly the case for *PT*-symmetric acoustics in which the electrical control can easily move the system in or out of the desired *PT* symmetric

state.²⁹ Other examples include a non-invasive, shadow-free, fully invisible acoustic sensor, based on a *PT*-symmetric distribution of balanced gain and loss;²⁷ non-reciprocal transmission controlled by subwavelength nonlinear, asymmetric structure over a relatively broad frequency range.⁴⁵

LOW COST MANUFACTURING AS THE ENABLING NEXT STEP

For large-scale applications, low cost mass manufacturing is an inevitable step. However, precisely in this area, the development of acoustic metamaterial meets its major hurdle, since acoustic metamaterials mostly involve complex designed structures, sometimes involving multiple materials with different material parameters, and usually conceived without the consideration of simple or low-cost manufacturing. It is fortuitous that 3D printing has arrived on the scene at about the same time as the development of acoustic metamaterials. Many of the experimental samples, most involving only one material but with complex geometries, were fabricated by 3D printing.^{58,59} However, 3D printing is still too expensive for mass manufacturing, and the use of multiple material components may pose a challenge. However, even though 3D printing is not yet a viable mass production tool, some of its design logic may have infiltrated into the mass manufacturing technology, so that new developments may happen in the near future to close this gap. When that happens, the acoustic metamaterial may enter an entirely new development stage, with the demands of the mass market serving as one of its drivers.

ACKNOWLEDGMENTS

Y.W. wishes to acknowledge funding support from King Abdullah University of Science and Technology BAS/1/1626-01-01. P.S. wishes to acknowledge funding support from Hong Kong Government Grant Nos. AoE/P-02/12 and ITF UIM292.

¹Z. Liu, X. Zhang, Y. Mao, Y. Y. Zhu, Z. Yang, C. T. Chan, and P. Sheng, *Science* **289**(5485), 1734–1736 (2000).

²S. A. Cummer, J. Christensen, and A. Alù, *Nat. Rev. Mater.* **1**, 16001 (2016).

- ³G. Ma and P. Sheng, *Sci. Adv.* **2**(2), e1501595 (2016).
- ⁴P. A. Deymier, *Acoustic Metamaterials and Phononic Crystals* (Springer Science & Business Media, 2013).
- ⁵P. F. Pai and G. Huang, *Theory and Design of Acoustic Metamaterials*. (SPIE, 2015).
- ⁶M. Yang and P. Sheng, *Annu. Rev. Mater. Res.* **47**, 83–114 (2017).
- ⁷U. Leonhardt, *Science* **312**(5781), 1777–1780 (2006).
- ⁸J. B. Pendry, D. Schurig, and D. R. Smith, *Science* **312**(5781), 1780–1782 (2006).
- ⁹H. Chen and C. T. Chan, *Appl. Phys. Lett.* **91**(18), 183518 (2007).
- ¹⁰W. M. Graeme, *New J. Phys.* **9**(10), 359 (2007).
- ¹¹C. Huanyang and C. T. Chan, *J. Phys. D: Appl. Phys.* **43**(11), 113001 (2010).
- ¹²Y. Zhang, Y.-W. Tan, H. L. Stormer, and P. Kim, *Nature* **438**(7065), 201–204 (2005).
- ¹³K. S. Novoselov, A. K. Geim, S. V. Morozov, D. Jiang, M. I. Katsnelson, I. V. Grigorieva, S. V. Dubonos, and A. A. Firsov, *Nature* **438**(7065), 197–200 (2005).
- ¹⁴X. Zhang and Z. Liu, *Phys. Rev. Lett.* **101**(26), 264303 (2008).
- ¹⁵D. Torrent and J. Sánchez-Dehesa, *Phys. Rev. Lett.* **108**(17), 174301 (2012).
- ¹⁶J. Mei, Y. Wu, C. T. Chan, and Z.-Q. Zhang, *Phys. Rev. B* **86**(3), 035141 (2012).
- ¹⁷J. Lu, C. Qiu, M. Ke, and Z. Liu, *Phys. Rev. Lett.* **116**(9), 093901 (2016).
- ¹⁸S.-Y. Yu, X.-C. Sun, X. Ni, Q. Wang, X.-J. Yan, C. He, X.-P. Liu, L. Feng, M.-H. Lu, and Y.-F. Chen, *Nat. Mater.* **15**(12), 1243–1247 (2016).
- ¹⁹S. H. Mousavi, A. B. Khanikaev, and Z. Wang, *Nat. Commun.* **6**, 8682 (2015).
- ²⁰R. Fleury, D. L. Sounas, C. F. Sieck, M. R. Haberman, and A. Alù, *Science* **343**(6170), 516–519 (2014).
- ²¹X. Ni, C. He, X.-C. Sun, X.-P. Liu, M.-H. Lu, L. Feng, and Y.-F. Chen, *New J. Phys.* **17**(5), 053016 (2015).
- ²²Z. Yang, F. Gao, X. Shi, X. Lin, Z. Gao, Y. Chong, and B. Zhang, *Phys. Rev. Lett.* **114**(11), 114301 (2015).
- ²³A. B. Khanikaev, R. Fleury, S. H. Mousavi, and A. Alù, *Nat. Commun.* **6**, 8260 (2015).
- ²⁴P. Wang, L. Lu, and K. Bertoldi, *Phys. Rev. Lett.* **115**(10), 104302 (2015).
- ²⁵Z.-G. Chen and Y. Wu, *Phys. Rev. Appl.* **5**(5), 054021 (2016).
- ²⁶X. Zhu, H. Ramezani, C. Shi, J. Zhu, and X. Zhang, *Phys. Rev. X* **4**(3), 031042 (2014).
- ²⁷R. Fleury, D. Sounas, and A. Alù, *Nat. Commun.* **6**, 5905 (2015).
- ²⁸J. Christensen, M. Willatzen, V. R. Velasco, and M. H. Lu, *Phys. Rev. Lett.* **116**(20), 207601 (2016).
- ²⁹C. Shi, M. Dubois, Y. Chen, L. Cheng, H. Ramezani, Y. Wang, and X. Zhang, *Nat. Commun.* **7**, 11110 (2016).
- ³⁰Y. Aurégan and V. Pagneux, *Phys. Rev. Lett.* **118**(17), 174301 (2017).
- ³¹G. Ma, M. Yang, S. Xiao, Z. Yang, and P. Sheng, *Nat. Mater.* **13**(9), 873–878 (2014).
- ³²J. Mei, G. Ma, M. Yang, Z. Yang, W. Wen, and P. Sheng, *Nat. Commun.* **3**, 756 (2012).
- ³³B. Liang, B. Yuan, and J.-C. Cheng, *Phys. Rev. Lett.* **103**(10), 104301 (2009).
- ³⁴B. Liang, X. S. Guo, J. Tu, D. Zhang, and J. C. Cheng, *Nat. Mater.* **9**(12), 989–992 (2010).
- ³⁵S. A. Cummer, *Science* **343**(6170), 495–496 (2014).
- ³⁶X.-F. Li, X. Ni, L. Feng, M.-H. Lu, C. He, and Y.-F. Chen, *Phys. Rev. Lett.* **106**(8), 084301 (2011).
- ³⁷H. Jia, M. Ke, C. Li, C. Qiu, and Z. Liu, *Appl. Phys. Lett.* **102**(15), 153508 (2013).
- ³⁸C. Shen, Y. Xie, J. Li, S. A. Cummer, and Y. Jing, *Appl. Phys. Lett.* **108**(22), 223502 (2016).
- ³⁹Z.-M. Gu, B. Liang, X.-Y. Zou, J. Yang, Y. Li, J. Yang, and J.-C. Cheng, *Appl. Phys. Lett.* **107**(21), 213503 (2015).
- ⁴⁰A. A. Maznev, A. G. Every, and O. B. Wright, *Wave Motion* **50**(4), 776–784 (2013).
- ⁴¹C. He, X. Ni, H. Ge, X.-C. Sun, Y.-B. Chen, M.-H. Lu, X.-P. Liu, and Y.-F. Chen, *Nat. Phys.* **12**(12), 1124–1129 (2016).
- ⁴²J. Mei, Z. Chen, and Y. Wu, *Sci. Rep.* **6**, 32752 (2016).
- ⁴³Z. Zhang, Q. Wei, Y. Cheng, T. Zhang, D. Wu, and X. Liu, *Phys. Rev. Lett.* **118**(8), 084303 (2017).
- ⁴⁴J. Lu, C. Qiu, L. Ye, X. Fan, M. Ke, F. Zhang, and Z. Liu, *Nat. Phys.* **13**(4), 369–374 (2017).
- ⁴⁵B.-I. Popa and S. A. Cummer, *Nat. Commun.* **5**, 3398 (2014).
- ⁴⁶J. J. Park, C. M. Park, K. J. B. Lee, and S. H. Lee, *Appl. Phys. Lett.* **106**(5), 051901 (2015).
- ⁴⁷J. Zhao, B. Li, Z. N. Chen, and C.-W. Qiu, *Appl. Phys. Lett.* **103**(15), 151604 (2013).
- ⁴⁸Y. Li, X. Jiang, R.-Q. Li, B. Liang, X.-Y. Zou, L.-L. Yin, and J.-C. Cheng, *Phys. Rev. Appl.* **2**(6), 064002 (2014).
- ⁴⁹M. Jun and W. Ying, *New J. Phys.* **16**(12), 123007 (2014).
- ⁵⁰Y. Li, X. Jiang, B. Liang, J.-C. Cheng, and L. Zhang, *Phys. Rev. Appl.* **4**(2), 024003 (2015).
- ⁵¹X. Yang, J. Yin, G. Yu, L. Peng, and N. Wang, *Appl. Phys. Lett.* **107**(19), 193505 (2015).
- ⁵²J. Li, W. Wang, Y. Xie, B.-I. Popa, and S. A. Cummer, *Appl. Phys. Lett.* **109**(9), 091908 (2016).
- ⁵³Y. Li, C. Shen, Y. Xie, J. Li, W. Wang, S. A. Cummer, and Y. Jing, *Phys. Rev. Lett.* **119**(3), 035501 (2017).
- ⁵⁴Z. Liang and J. Li, *Phys. Rev. Lett.* **108**(11), 114301 (2012).
- ⁵⁵Y. Li, B. Liang, X.-Y. Zou, and J.-C. Cheng, *Appl. Phys. Lett.* **103**(6), 063509 (2013).
- ⁵⁶Y. Xie, A. Konneker, B.-I. Popa, and S. A. Cummer, *Appl. Phys. Lett.* **103**(20), 201906 (2013).
- ⁵⁷M. Molerón, M. Serra-García, and C. Daraio, *Appl. Phys. Lett.* **105**(11), 114109 (2014).
- ⁵⁸Y. Xie, W. Wang, H. Chen, A. Konneker, B.-I. Popa, and S. A. Cummer, *Nat. Commun.* **5**, 5553 (2014).
- ⁵⁹Y. Cheng, C. Zhou, B. G. Yuan, D. J. Wu, Q. Wei, and X. J. Liu, *Nat. Mater.* **14**(10), 1013–1019 (2015).
- ⁶⁰K. Tang, C. Qiu, J. Lu, M. Ke, and Z. Liu, *J. Appl. Phys.* **117**(2), 024503 (2015).
- ⁶¹Y. Li and B. M. Assouar, *Appl. Phys. Lett.* **108**(6), 063502 (2016).
- ⁶²R. A. Jahdali and Y. Wu, *Appl. Phys. Lett.* **108**(3), 031902 (2016).
- ⁶³Y. Tian, Q. Wei, Y. Cheng, and X. Liu, *Appl. Phys. Lett.* **110**(19), 191901 (2017).
- ⁶⁴S. Qi, Y. Li, and B. Assouar, *Phys. Rev. Appl.* **7**(5), 054006 (2017).
- ⁶⁵M. Yang, Y. Li, C. Meng, C. Fu, J. Mei, Z. Yang, and P. Sheng, *C. R. Méc.* **343**(12), 635–644 (2015).
- ⁶⁶A. Merkel, G. Theocharis, O. Richoux, V. Romero-García, and V. Pagneux, *Appl. Phys. Lett.* **107**(24), 244102 (2015).
- ⁶⁷V. Leroy, A. Strybulevych, M. Lanoy, F. Lemoult, A. Tourin, and J. H. Page, *Phys. Rev. B* **91**(2), 020301 (2015).
- ⁶⁸C. Meng, X. Zhang, S. T. Tang, M. Yang, and Z. Yang, *Sci. Rep.* **7**, 43574 (2017).
- ⁶⁹M. Yang, C. Meng, C. Fu, Y. Li, Z. Yang, and P. Sheng, *Appl. Phys. Lett.* **107**(10), 104104 (2015).
- ⁷⁰V. Romero-García, G. Theocharis, O. Richoux, A. Merkel, V. Tournat, and V. Pagneux, *Sci. Rep.* **6**, 19519 (2016).
- ⁷¹X. Cai, Q. Guo, G. Hu, and J. Yang, *Appl. Phys. Lett.* **105**(12), 121901 (2014).
- ⁷²X. Jiang, B. Liang, R.-Q. Li, X.-Y. Zou, L.-L. Yin, and J.-C. Cheng, *Appl. Phys. Lett.* **105**(24), 243505 (2014).
- ⁷³N. Jiménez, V. Romero-García, V. Pagneux, and J.-P. Groby, *Phys. Rev. B* **95**(1), 014205 (2017).
- ⁷⁴D. Ye, Z. Wang, K. Xu, H. Li, J. Huangfu, Z. Wang, and L. Ran, *Phys. Rev. Lett.* **111**(18), 187402 (2013).
- ⁷⁵Y. P. Lee, J. Y. Rhee, Y. J. Yoo, and K. W. Kim, *Metamaterials for Perfect Absorption* (Springer, 2016).
- ⁷⁶M. Yang, S. Chen, C. Fu, and P. Sheng, *Mater. Horiz.* **4**, 673 (2017).
- ⁷⁷B.-I. Popa, L. Zigoneanu, and S. A. Cummer, *Phys. Rev. B* **88**(2), 024303 (2013).
- ⁷⁸A. Baz, *New J. Phys.* **11**(12), 123010 (2009).
- ⁷⁹W. Akl and A. Baz, *J. Intell. Mater. Syst. Struct.* **21**(5), 541–556 (2010).